Research Article

Received: 5 July 2011 Revised: 16 October 2011 Accepted: 12 December 2011 Published online in Wiley Online Library: 10 May 2012

(wileyonlinelibrary.com) DOI 10.1002/pi.4188

Enhanced mechanical and thermal properties of rigid polyurethane foam composites containing graphene nanosheets and carbon nanotubes

Dingxiang Yan,[a] Ling Xu,[a] Chen Chen,[b]* Jianhua Tang,[c] Xu Ji[c]* and Zhongming Li[a]

Abstract

The comparative study of rigid polyurethane foam (RPUF) nanocomposites based on graphene nanosheets (GNSs) and carbon nanotubes (CNTs) has been reported. A GNS content of 0.3 wt% in polyol turns to be optimal for its foamability with the isocyanate component, as verified by rheology measurements. Scanning electron microscopy and transmission electron microscopy observations reveal a homogeneous dispersion of GNSs and CNTs in the RPUF nanocomposites. Only 0.3 wt% loading of GNSs and CNTs led to 36% and 25% improvement respectively in the compressive modulus of the RPUF nanocomposites. Meanwhile, 16 °C and 14 °C improvements in the glass transition temperature confirm the important role of both the nanofillers in the heat resistance of RPUF nanocomposites. These results additionally indicate that GNSs work more effectively than CNTs in mechanical property and heat resistance enhancement of the RPUF nanocomposites. The superiority of GNSs over CNTs can be attributed to their wrinkled surface structure, unique two-dimensional geometrical morphology and higher specific surface area, which results in stronger interaction and restriction of segmental motion at the interface between the GNSs and the RPUF matrix. In addition, changes in the thermal conductivity of the nanocomposites are negligible, indicating that incorporation of GNSs and CNTs will not hinder the application of RPUF nanocomposites as thermal insulators. On the contrary, the enhancement in mechanical properties and heat resistance will undoubtedly expand the application range of polyurethane foam materials.

Keywords: graphene nanosheets; carbon nanotubes; rigid polyurethane foam; nanocomposites; compressive properties; heat resistance

INTRODUCTION

Rigid polyurethane foam (RPUF), with excellent thermal insulation, electrical insulation and chemical resistance, is extensively used for insulation in refrigerators, construction materials and chemical pipelines.[1,2] As one of the most popular polyurethane products, another advantage of RPUF is its low density owing to its porous structure, which makes it possible to economize in raw material. However, the mechanical properties and heat resistance of pristine RPUF are usually unsatisfactory due to the sandwich structure with a weak core, especially for structural and semi-structural applications.[3,4] Therefore, a great deal of effort has been devoted to improving the physical properties and heat resistance of RPUF, and for this the manufacture of nanofiller-modified RPUF nanocomposites works effectively.[5–10]

Nanofillers, with enormous specific surface area and outstanding physical properties, have stronger interfacial adhesion with the polymer matrix compared with conventional fillers. Therefore they are usually expected to functionalize RPUF materials, aiming to achieve excellent performance.[11] For instance, addition of 1.0 wt% nanoclay into RPUF increased its compressive modulus and strength by 20% and 38%; moreover, the same loading of carbon nanofibers led to an increase of 40% and 57%, respectively.[4] Improvements in heat resistance have also been achieved with the inclusion of various nanoparticles such as silicon carbide and titanium dioxide.[7]

Graphene nanosheets (GNSs), as a carbon allotrope a single atom or several atoms thick, have been demonstrated to have outstanding mechanical, electrical and thermal properties.[12] Due to these unique properties, GNSs were reported to have potential applications in the preparation of nano-modified materials with excellent overall performance.[13–15] Since the pioneering research on conductive-graphene-filled polystyrene,[16] considerable attention has been paid to GNS-based polymer nanocomposites

* *Correspondence to: Chen Chen, Analytical and Testing Center, Sichuan University, Chengdu 610065, Sichuan, PR China. E-mail: cdcc@scu.edu.cn*

Xu Ji, College of Chemical Engineering, Sichuan University, Chengdu 610065, Sichuan, PR China. E-mail: jxhhpb@163.com

a *College of Polymer Science and Engineering, State Key Laboratory of Polymer Materials Engineering, Sichuan University, Chengdu 610065, Sichuan, PR China*

b *Analytical and Testing Center, Sichuan University, Chengdu 610065, Sichuan, PR China*

c *College of Chemical Engineering, Sichuan University, Chengdu 610065, Sichuan, PR China*

with the purpose of obtaining functional materials of high performance.[17–19] Recently, Vadukumpully *et al.*[20] reported a significant enhancement in the mechanical properties of pure poly(vinyl chloride) films with 2.0 wt% loading of graphene, such as a 58% and 130% increase in Young's modulus and tensile strength, respectively. In addition, a 20 °C increase in the glass transition temperature served as evidence for the enhanced heat resistance with the introduction of graphene. A similar enhancement effect also existed in silicone foam nanocomposites.[21] As reported, 0.25 wt% functionalized graphene sheet increased the normalized modulus of filled foam by over 200% compared with the control silicone foam sample.[21]

Another type of carbonous nanofiller, carbon nanotubes (CNTs), have been proved to be superb reinforcement nanofillers for various polymer nanocomposites in improving their mechanical, electrical and thermal properties.[22] CNTs and GNSs are both made up of graphite monolayers, i.e. they have the same fundamental structural unit. The most distinct difference lies in their geometrical morphology, e.g. several graphite monolayers stack into two-dimensional nanoplate-like GNSs or roll into one-dimensional nanoline-like CNTs.[23] Generally, physical and mechanical properties of polymer nanocomposites are greatly influenced by the geometrical morphology of the nanofillers.[24–28] For instance, at a nanofiller weight fraction of 0.1% ±0.002%, the Young's modulus of a graphene platelet nanocomposite was *ca* 31% greater than that of the pristine epoxy, compared with an improvement of *ca* 3% for a single-walled CNT-based nanocomposite. The superiority of graphene platelets over CNTs in terms of mechanical property enhancement can be related to their high specific surface area, enhanced nanofiller–matrix adhesion/interlocking arising from their wrinkled (rough) surface as well as the two-dimensional (planar) geometry of graphene platelets.[24] Moreover, graphene-based nanocomposites were also found to be more efficient thermal conductors than CNT nanocomposites owing to smaller Kapitza resistance and the geometry of the graphene sheet.[27] In our recent work, polystyrene containing GNSs were more effective in the formation of conductive networks in the polystyrene melt than CNTs.[29] In the current work, the aim was to obtain high-performance RPUF nanocomposites filled with GNSs and CNTs. Compared with solid materials, the marked characteristics of foam materials are their porous structure. The addition of nanofillers and their dispersion (in the cell walls or cell struts) both have an influence on the foam process, impacting on the formation of the porous structure and thus the final performance of the foam materials. Because of the distinct difference existing in their geometrical morphology, it is of great importance to comparatively study the foamability and porous structure–performance relationship of RPUF nanocomposites with two-dimensional GNSs and one-dimensional CNTs. Therefore, mechanical and dynamic mechanical thermal analyses were introduced to elucidate the effect of the geometry of the nanofillers on the mechanical and thermal properties of the nanocomposites. Results demonstrate that GNSs are superior nanofillers to CNTs for improving both the mechanical and thermal properties of RPUF, highlighting the application of graphene in polymer foam nanocomposites. Furthermore, this work is expected to help us further understand the performance of polymer nanocomposites reinforced with different dimensional carbon nanofillers.

EXPERIMENTAL

Materials

Graphene oxide (GO) was synthesized from expanded graphite by the modified 'Hummers' method, with a thickness of 1–2 nm and an average calculated length of 0.87 μm, as described in our previous work.[25,30] CNTs used here were carboxyl multiwall CNTs with a purity of > 95 wt% and were produced by the Nano Harbor Co. Ltd (Chengdu, China) via the chemical vapour deposition method, with a diameter of 30–50 nm and a length of about 20 μm. The polyether polyol, Model GR-4110, originating from polypropylene oxide and sucrose/glycerin base, was obtained from HongQiao Petro. Co. (Shanghai, China) and the isocyanate N200 was purchased from ChangFeng Petro. Co. (Chongqing, China). Silicone glycol copolymer Niax L-580 was used as a surfactant, and the catalyst used contained triethylene diamine and stannous octoate. The blowing agent was distilled water.

Preparation of GNS- and CNT-filled RPUF nanocomposites

GO was suspended in distilled water (1 mg mL^{-1}) with strong stirring and ultrasonication (400 W power and 40 kHz frequency) to create a homogeneous dispersion, and the dehydrated polyether polyol was added to the dispersion. The mixture was subsequently sonicated at 30 °C for 1 h to reach a uniform dispersion of GO in the polyol. Then the temperature was increased to 95 °C for 3 h in the presence of hydrazine hydrate. The hydrazine hydrate was an effective reducing agent which converted GO to GNS; the weight ratio of hydrazine hydrate to GO was 1. With the aid of ultrasonication and stirring, a homogeneous GNS/polyol/distilled water dispersion was obtained. Subsequently, the distilled water was evaporated to constant weight and the additive (0.2 wt% surfactant and 0.1 wt% catalyst) was added to the GNS/polyol mixture, which was then stirred until a uniform mixture was obtained. Finally, the isocyanate (weight ratio of polyol/isocyanate 100/180) was added and stirred for an additional 15 s. The foams were then transferred to a mould with a lid, expanded to fill the entity and post-cured in an oven at 100 °C for 4 h. In this work, the density of all RPUF nanocomposites was fixed at about 200 kg m^{-3}. Foams containing 0.1, 0.2 and 0.3 wt% of GNSs were produced. For comparison, CNTs were also introduced to the same content. The procedure for processing pure RUPF was started from the addition of the additive into dehydrated polyether polyol and the following procedure was the same as with the preparation of GNS-filled RPUF nanocomposites.

Characterization

Rheological behaviours of dispersions were evaluated at 20 °C using a rotating rheometer AR 2000ex from TA Instruments (USA) with parallel plate geometry (with strains of 1% and gap of 1000 μm).

The morphology of the samples was observed in a JSM-9600 (JEOL, Japan) scanning electron microscope with an accelerating voltage of 20 kV. Transmission electron microscopy (TEM) images were obtained with a Philips T20ST electron microscope (Amsterdam, Netherland) at an acceleration voltage of 200 kV. The nanocomposite samples were prepared with a thickness of 50–60 nm via a microtome.

The compressive strength and the compressive modulus were measured with a universal electronic tensile machine (Shimadzu, Japan) with compression rate of 2 mm min^{-1} according to ASTM D 1621-94. The specimens for measurement were machined into dimensions of 50 × Φ50 mm^3. To eliminate the discrepancies

aroused by the foam density, the compressive strength and modulus values were normalized to a density of 200 kg m^{-1} using the following equations, which are derived from the geometric model of closed-cell foam proposed by Gibson and Ashby.[31]

$$\sigma_n = \sigma_m \left(\frac{200}{\rho}\right)^2 \left(\frac{1+\sqrt{200/\rho_s}}{1+\sqrt{\rho/\rho_s}}\right)^2 \quad (1)$$

$$E_n = E_m \frac{\phi^2\left(\frac{200}{\rho_s}\right)^2 + (1-\phi)\left(\frac{200}{\rho_s}\right)}{\phi^2\left(\frac{\rho}{\rho_s}\right)^2 + (1-\phi)\left(\frac{\rho}{\rho_s}\right)} \quad (2)$$

where σ_n and E_n are the normal compressive strength and modulus; σ_m and E_m are the measured compressive strength and modulus; ρ is the observed density of the RPUF in kg m^{-3}; ρ_s is the density of solid polyurethane with a value of 1200 kg m^{-1}; and ϕ is the fraction of polymer contained in the cell struts with a value of 0.9. X-ray photoelectron spectroscopy (XPS) analyses were performed with an XSAM800 (Kratos Company, UK) using Al Kα radiation ($h\nu = 1486.6$ eV).

Dynamical mechanical analysis (DMA) was carried out using a Q800 DMA instrument (TA Instruments) with a heating rate of 3 °C min^{-1} from 50 to 250 °C. The dimensions of the samples were 35 × 10 × 4 mm^3.

Thermal conductivity was measured by the transient plane source technique using a hot disc 2500-OT equipment at room temperature according to ASTM C518-91.

RESULTS AND DISCUSSION

Rheology and foamability of polyol nanodispersions

Figure 1 shows the steady shear behaviours of GNS- and CNT-filled polyol nanodispersions. It can be seen that the pristine polyol flows in a Newtonian manner, the CNT nanodispersion shows moderate shear thinning, while the GNS nanodispersion exhibits distinct shear thinning. The physical restraints of polyol chains resulting from the interaction between polyol chains and GNSs or CNTs in the nanodispersions are assumed to be the key points for shear thinning.[21,32] At the same loading (0.3 wt%), the GNS nanodispersion displays stronger shear thinning than the CNT nanodispersion, indicating that two-dimensional GNSs have a stronger restriction effect on polyol molecular chains than one-dimensional CNTs, which can be attributed to the wrinkled surface structure of GNSs and their unique two-dimensional geometrical morphology with higher specific surface area than that of CNTs.[24] Moreover, compared with pristine polyol, for example, at a shear rate of 10 s^{-1} the relative viscosities of 0.3 wt% GNS/polyol and CNT/polyol nanodispersions are approximately 3.1 and 1.4, respectively. These moderate increases in viscosity would not hinder the foamability of polyol with the isocyanate component.[33] However, the relative viscosity of 0.5 wt% GNS/polyol nanodispersion increases to 15.4 and the nanodispersion might be difficult to process into foam.[6]

Figure 2 shows the linear viscoelastic properties of GNS- and CNT-filled polyol nanodispersions to further reveal the effect of GNSs and CNTs on the foamability of polyol with isocyanate. Apparently, the storage modulus G' of both the nanodispersions continuously increases with frequency, indicating that 0.3 wt% of GNSs and CNTs are not enough to construct a complete network structure. Moreover, the storage modulus G' of 0.3 wt% GNS nanodispersion is significantly higher than that of CNT nanodispersion, which also testifies to the stronger interaction between polyol and GNSs. When the GNS content increases to 0.5 wt%, the storage modulus becomes independent of frequency and the nanodispersion exhibits a solid-like linear viscoelastic behaviour, suggesting development of a highly crosslinked three-dimensional network structure,[34,35] which is supposed to hinder the foaming process. The above results suggest that the geometrical morphology of carbon nanofillers has a significant effect on the rheology and foamability of polyol nanodispersions.[36,37] GNSs with a two-dimensional structure cause higher steady viscosity and storage modulus than CNTs with a one-dimensional structure, resulting in a difficult foaming process, and thus the loading of GNSs should not be higher than 0.3 wt% in RPUF.

Cell morphology of RPUF nanocomposites

Figure 3 shows the typical closed cellular structure of RPUF. The cell size and cell density for pristine RPUF are 165 μm and 3.6 × 10^5 cells cm^{-3}. Addition of 0.3 wt% GNSs decreases the cell size to 145 μm and increases the cell density to 5.3 × 10^5 cells cm^{-3}, while the same loading of CNTs results in 161 μm and 3.8 × 10^5 cells cm^{-3}, respectively. These results are indicative of a moderate heterogeneous nucleation effect of GNSs on foaming while the heterogeneous nucleation effect of CNTs is negligible in comparison with the nucleation of common ultra-fine particles for RPUF.[38] With high specific surface area and strong interfacial interaction as confirmed by the rheological properties, GNSs

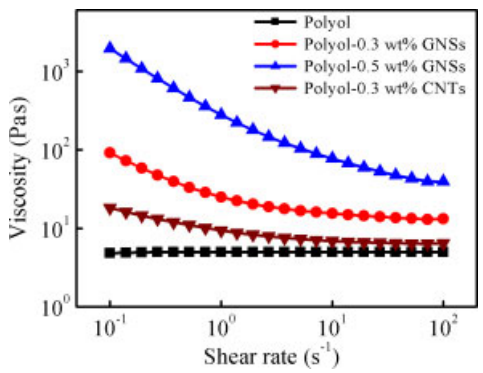

Figure 1. Steady shear viscosities of GNS- and CNT-filled polyol nanodispersions.

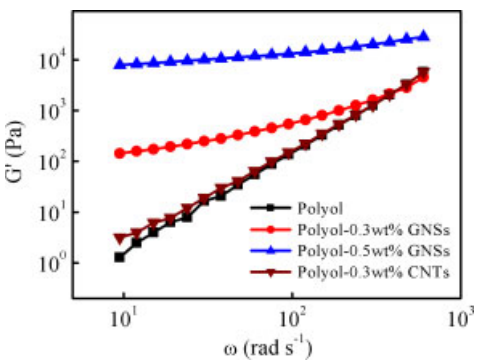

Figure 2. Linear viscoelastic properties of GNS- and CNT-filled polyol nanodispersions.

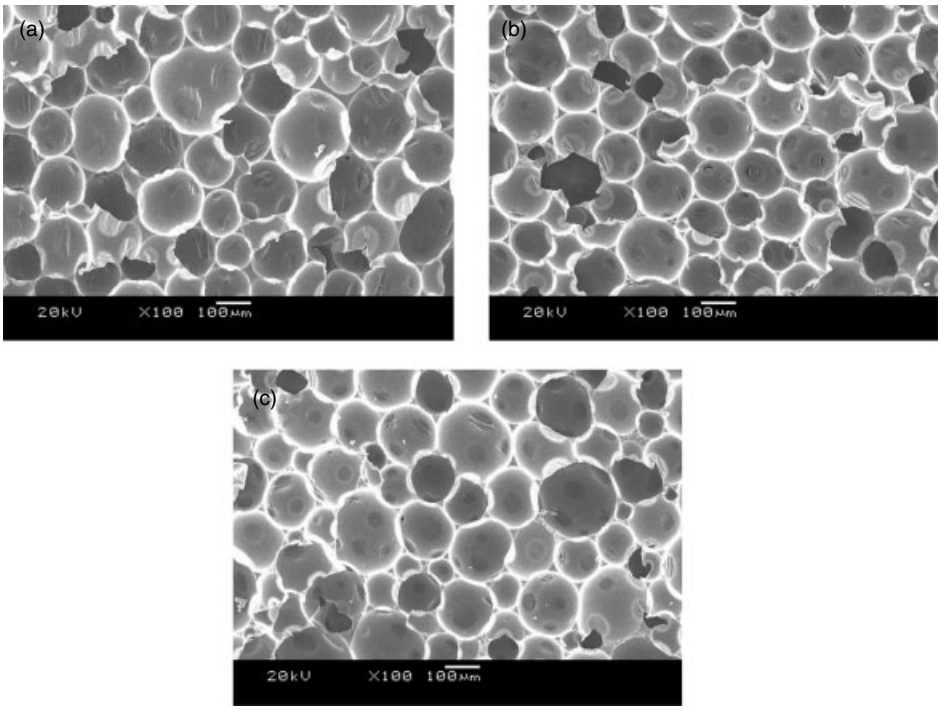

Figure 3. SEM micrographs of (a) pristine RPUF, (b) GNS/RPUF nanocomposite with 0.3 wt% GNSs and (c) CNT/RPUF nanocomposite with 0.3 wt% CNTs.

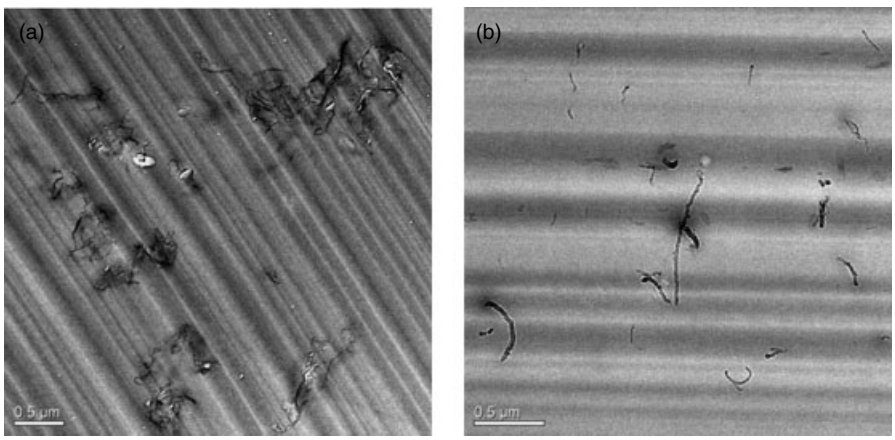

Figure 4. Representative TEM micrographs of (a) GNS/RPUF nanocomposite with 0.3 wt% GNSs and (b) CNT/RPUF nanocomposite with 0.3 wt% CNTs.

should be more conducive to reducing the nucleation free energy to create effective nucleation sites than CNTs.[38,39] Nevertheless, due to the drastic rise in flow viscosity at a higher GNS loading, the GNS loading is not allowed to be more than 0.3 wt%; hence, the effective nucleation sites are not enough to decrease the cell size significantly.

Figure 4 shows TEM micrographs of the GNS and CNT nanocomposites. A desirable dispersion is obtained for the two nanofillers, where hardly any aggregates are observed. Thanks to oxygen functional groups (e.g. hydroxyl, epoxide, carboxyl and carbonyl groups) on the basal planes and edges, GO is strongly hydrophilic and easy to homogeneously disperse in distilled water in the form of individual or multiple layers, with the aid of ultrasonication. During the reduction process, GO is converted to GNSs, which are then wrapped with the aid of ultrasonication to prevent aggregation upon evaporation of water.[40] In the following *in situ* polymerization, a desirable dispersion of GNSs in the RPUF can be achieved and the wrinkled structure is generated via covalent bond interaction between isocyanate and residual oxygen functional groups in the GNSs.[41,42] A homogeneous dispersion of CNTs in RPUF is also obtained under continuous ultrasonication, as described in our previous work.[9,43] The favourable dispersion of GNSs and CNTs in RPUF is particularly crucial for enhancement of the mechanical and thermal properties of RPUF, which will be discussed in the following sections.

Mechanical properties of RPUF nanocomposites

Given their significant application as foam materials, the compressive property of RPUF is a critical property, which is shown in Fig. 5. The compressive strength and modulus increase reasonably with the amount of GNSs and CNTs. For example, the compressive strength and modulus increase by 32% and 36% respectively from 3.1 MPa and 73.8 MPa for pristine RPUF to 4.1 MPa and 100.1 MPa for 0.3 wt% GNS nanocomposite, while the values for 0.3 wt% CNT

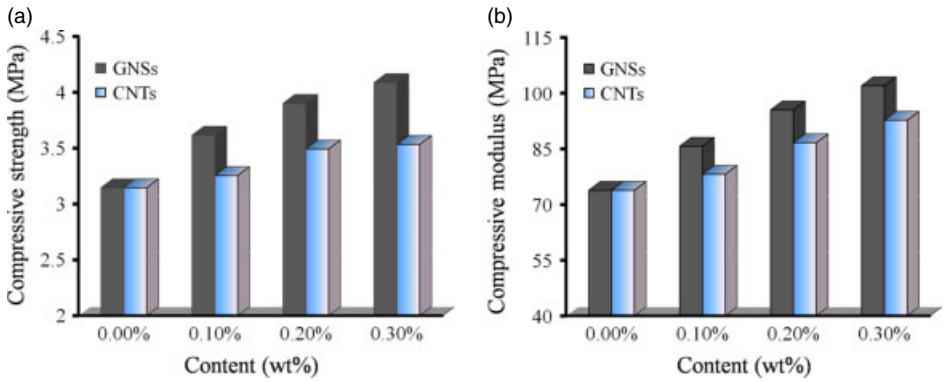

Figure 5. Compressive strength (a) and compressive modulus (b) of various GNS- and CNT-filled RPUF nanocomposites.

nanocomposite are 16% and 25%. Compared with other nanofiller (such as nanoclay or carbon nanofibre) RPUF composites,[4,6] e.g. RPUF nanocomposite based on 0.43 wt% carbon nanofibres exhibited only 16% improvement in normalized compressive modulus,[6] GNSs and CNTs are undoubtedly more efficient.

The Halpin–Tsai model, which is widely used for predicting the modulus of distributed filler-reinforced solid composites,[44,45] in conjunction with the Gibson–Ashby model for the modulus of closed-cell foams, is introduced to estimate the modulus of the GNS- and CNT-filled RPUF composites.

$$E_{FC} = E_{PU}\left[\frac{1+\eta_L \xi V_{filler}}{1-\eta_L V_{filler}}\right]\left[\phi^2\left(\frac{\rho_n}{\rho_s}\right)^2 + (1-\phi)\left(\frac{\rho_n}{\rho_s}\right)\right] \quad (3)$$

$$\eta_L = \frac{(E_{filler}/E_{PU})-1}{(E_{filler}/E_{PU})+\xi} \quad (4)$$

where E_{FC} and E_{PU} are the modulus of the RPUF composite and solid polyurethane, respectively. E_{filler} represents the modulus of GNSs or CNTs. V_{filler} is the volume fraction of GNSs or CNTs in the solid part of the RPUF. ρ_n and ρ_s are the normal density of RPUF and solid which are 200 and 1200 kg m^{-3}, respectively. For the GNS composite, $\xi = (2/3)(l/t)_{GNS}$, where l and t refer to the length and thickness of the GNSs and are about 500 nm and 0.34 nm.[46] For the CNT composite, $\xi = 2(l/d)_{CNT}$, where l and d refer to the length and diameter of the CNTs and are about 20 μm and 40 nm, respectively. The moduli of the GNSs and CNTs used here are about 750 and 400 GPa.[47–49] The modulus of pure solid polyurethane is 1.88 GPa from the experimental data, falling in the range of reported values for E_{PU} of 1.6 to 2.7 GPa.[50] The densities of GNSs and CNTs are 2200 and 2100 kg m^{-3}. The volume fractions of GNSs or CNTs in the solid part of the RPUF can be expressed as follows:

$$V_{filler} = \frac{\omega_{filler}}{\omega_{filler} + (\rho_{filler}/\rho_s)(1-\omega_{filler})} \quad (5)$$

where ω_{filler} is the weight fraction of GNSs or CNTs in the solid part of the RPUF composites. Substituting appropriate parameters into Eqns (3)–(5), the theoretical modulus of the RPUF composites can be estimated, as shown in Fig. 6.

It is found from Fig. 6 that the theoretical results are in good agreement with the experimental data, revealing outstanding enhancement effects of GNSs and CNTs on RPUF. The origin of the GNS and CNT reinforcement can be attributed to their ultra-high aspect ratio and powerful interfacial adhesion, which provide additional constraints to the segmental movement of the polymer

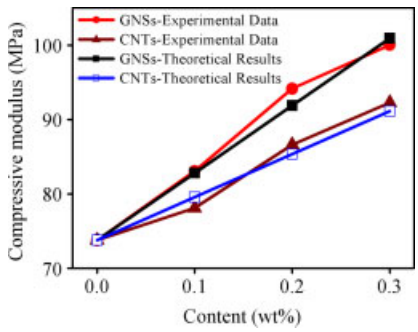

Figure 6. Normal experimental data of various GNS- and CNT-filled RPUF nanocomposites and calculated theoretical results derived from the Halpin–Tsai model in conjunction with the Gibson–Ashby model.

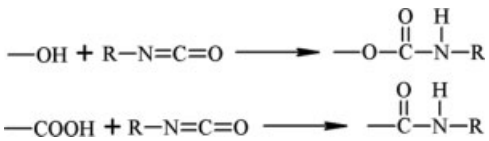

Scheme 1. Proposed reaction of hydroxyl and carboxyl with isocyanate to generate carbamate ester and amide.

Table 1. C/O atomic ratio and contents of oxygen-containing groups on GNSs and CNTs demonstrated by XPS measurements

Samples	C/O	–OH	O–C=O	C=O	C–O–C
GNSs	93.8/6.2	4.28%	0.79%	0.55%	0.30%
CNTs	97.6/2.4	1.56%	0.35%	0.22%	0.13%

chains and favour the efficient load transfer from the nanofillers to the matrix. The strong interfacial interaction is mainly aroused by the chemical reactions of the hydroxyl and carboxyl groups contained in GNSs and CNTs with isocyanate, which generate carbamate ester and amide,[42,51] as expressed in Scheme 1.

Additionally, Fig. 6 displays more effective reinforcement of GNSs than CNTs. The reasons may be as follows.[24] The wrinkled surface structure of GNSs is beneficial to their interfacial bonding with the matrix. The oxygen functional groups of GNSs are more than those of CNTs. More oxygen functional groups on the basal planes and edges of GNSs as demonstrated by XPS measurement (Table 1) bring out stronger chemical and hydrogen

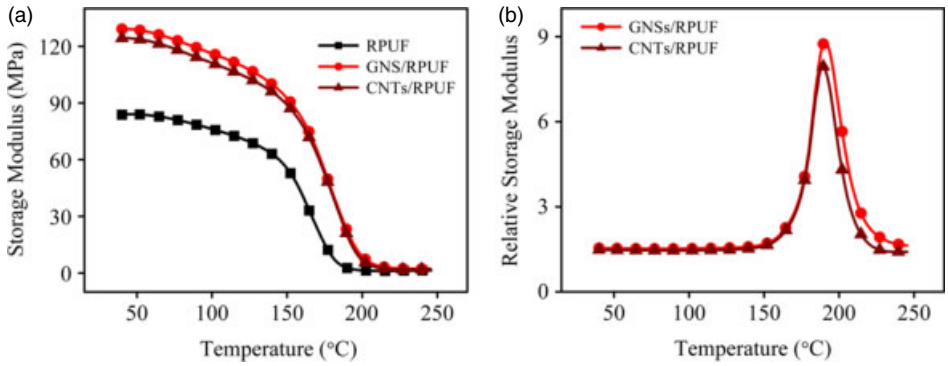

Figure 7. Temperature dependence of storage modulus (a) and relative storage modulus (b) for pristine RPUF and GNS- and CNT-filled RPUF nanocomposites with 0.3 wt% content.

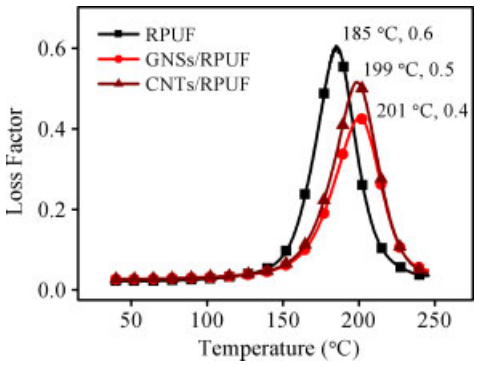

Figure 8. Temperature dependence of the loss factor (tan δ) for GNS- and CNT-filled RPUF nanocomposites with 0.3 wt% content.

bonding interactions between GNSs and the RPUF matrix; thus the interfacial interaction is more intense and the load transfers more easily. GNSs act as a more effective heterogeneous nucleating agent than CNTs, leading to a decrease in cell size. Finally, the unique two-dimensional geometrical morphology with a higher specific surface area of GNSs also contributes to the superior enhancement effect.

Dynamic mechanical thermal analysis of RPUF nanocomposites

Figure 7(a) shows the temperature dependence of the storage modulus (E') for pristine RPUF and GNS- and CNT-filled RPUF composites. E' for all samples decreases slowly and progressively with temperature in the initial stage and then shows a very strong decay between 180 and 210 °C, which correlates with the transition from the glassy to the rubbery state. In contrast to pristine RPUF, the improvement in E' for the GNS nanocomposite is more significant than that of the CNT nanocomposite. To better understand the effect of GNSs and CNTs on the storage modulus of the nanocomposites, the relative storage modulus is plotted as a function of temperature, as shown in Fig. 7(b). In the glassy region, 0.3 wt% GNSs or CNTs cause a minor rise in E', e.g. 54% and 48% improvement respectively at a temperature of 40 °C. In the glass transition region, the values increase sharply to 900% and 800% at about 190 °C. The marked improvement in storage modulus also suggests a favourable interfacial interaction between the nanofillers and the RPUF matrix.[20,52] In particular, the mobility of the polymer molecule chains near the glass transition temperature (T_g) is markedly confined, giving rise to an abrupt increase in storage modulus.

In the glass transition region, energy dissipation increases greatly as the loss factor (tan δ) peaks to a maximum, while the corresponding temperature maximum is considered to be T_g associated with α relaxation of the RPUF composites. Both T_g and tan δ interpret the mobility and movement capacity of polymer molecule chain segments. As presented in Figure 8, the apparent T_g and tan δ of pristine RPUF are 185 °C and 0.6, while the T_g shifts to 201 and 199 °C for GNS and CNT nanocomposites and tan δ shifts to 0.4 and 0.5, respectively. Undoubtedly, GNS and CNT loading induced an increase in T_g and a decrease in tan δ, demonstrating the stiffening barrier effect of these carbon nanofillers, i.e. the presence of GNSs and CNTs highly impedes the polymer chain motion via strong interfacial interactions and acts as a 'physical crosslink' during the glass transition,[21,53] which evidently improves the stiffness and heat resistance of the nanocomposites. Analogous to the compressive properties, the observed amplitude of the variation in T_g and tan δ is high for GNS nanocomposites compared with that of CNT nanocomposites, which is also ascribed to the greater interfacial interaction between the matrix RPUF and wrinkled GNSs with unique two-dimensional geometrical morphology. Furthermore, although tan δ decreases with addition of GNSs and CNTs, provided its value is larger than 0.3, damping effect should be considered to exist.

Thermal conductivity of RPUF nanocomposites

For application of foam nanocomposites as a thermal insulator material, the thermal conductivity is a crucial parameter. The thermal conductivity of pristine RPUF and 0.3 wt% GNS and CNT nanocomposites is shown in Table 2. A loading of 0.3 wt% GNSs slightly increases the thermal conductivity by 3% from 51.52×10^{-3} for pristine RPUF to 53.13×10^{-3} W m^{-1} K^{-1}, but only by 0.1% for CNTs. Two opposing factors could affect the thermal conductivity of RPUF nanocomposites.[2,21,54] On the one hand, the average cell size imposes a strong influence on the total thermal conductivity of the nanocomposites. It has been well established that thermal conductivity generally decreases with cell size. On the other hand, the thermal conductivity increases with incorporation of nanofillers with superior thermal conductivity. In this work, the cell size reduces a little with the existence of GNSs and CNTs, which is beneficial for the reduction of thermal conductivity. The increased thermal conductivity in the nanocomposites should therefore be ascribed to the superior thermal conductivity of GNSs and CNTs. Nevertheless, the increase in thermal conductivity is

Table 2. Thermal conductivity of GNS- and CNT-filled RPUF nanocomposites

Samples	Thermal conductivity ($\times 10^{-3}$ W m^{-1} K^{-1})
RPUF	51.52
0.3 wt% GNS/RPUF	53.13
0.3 wt% CNT/RPUF	51.57

very limited, which indicates that such loading of GNSs and CNTs would not hinder the application of RPUF nanocomposites as thermal insulator materials.

The current results indicate that RPUF nanocomposites with a very low loading of GNSs (0.3 wt%) could enhance the mechanical properties and heat resistance more than the same loading of CNTs. Due to the expensive manufacturing cost, impurities from catalysts, bundling and aggregation, industrial applications of CNTs are still limited.[14] In contrast, inexpensive and abundant raw materials along with a well-developed chemical oxidation reduction process make it cost-effective to manufacture GNSs. Because of the superiority of GNSs over CNTs in enhancing the mechanical properties and heat resistance of polymer nanocomposites, as observed by us and other researchers, GNSs are destined to serve as an alternative to CNTs to prepare high performance and multifunctional polymer nanocomposites.

CONCLUSIONS

RPUF nanocomposites containing satisfactorily dispersed GNSs and CNTs with enhanced mechanical properties and heat resistance have been obtained. Rheology measurements state that the preferable GNS content in polyol for its foamability with the isocyanate component should be 0.3 wt%. The observed cell morphology reveals that GNSs play a moderate role in the heterogeneous nucleation foaming process while the heterogeneous nucleation effect of CNTs is negligible. With only 0.3 wt% GNSs and CNTs, the improvements in compressive modulus are 36% and 25%, which are quite consistent with the results obtained from theoretical analysis by the Halpin–Tsai and Gibson–Ashby model, implying an outstanding enhancement effect of GNSs and CNTs. DMA results also reveal that the incorporation of GNSs improves the storage modulus and T_g more remarkably than that of CNTs. The superiority of GNSs over CNTs in terms of mechanical properties and heat resistance enhancement can be attributed to their wrinkled surface structure, unique two-dimensional geometrical morphology and higher specific surface area which results in stronger interface adhesion between the GNSs and RPUF.

ACKNOWLEDGEMENTS

The authors gratefully acknowledge financial support from the Nature Science Foundation of China (Grant No. 20976112, 20876099, 51121001) and State Key Laboratory for Modification of Chemical Fibers and Polymer Materials, Dong Hua University. Thanks are also given to Mr Zhu Li from the Analytical and Testing Center of Sichuan University for his help with the SEM measurements.

REFERENCES

1 Cao X, Lee LJ, Widya T and Macosko C, *Polymer* **46**:775–783 (2005).
2 Silva M, Takahashi J, Chaussy D, Belgacem M and Silva G, *J Appl Polym Sci* **117**:3665–3672 (2010).
3 Mondal P and Khakhar DV, *Macromol Symp* **216**:241–254 (2004).
4 Saha M, Kabir ME and Jeelani S, *Mater Sci Eng A* **479**:213–222 (2008).
5 Harikrishnan G, Patro TU and Khakhar D, *Ind Eng Chem Res* **45**:7126–7134 (2006).
6 Harikrishnan G, Singh SN, Kiesel E and Macosko CW, *Polymer* **51**:3349–3353 (2010).
7 Mahfuz H, Rangari VK, Islam MS and Jeelani S, *Composites Part A* **35**:453–460 (2004).
8 Verdejo R, Jell G, Safinia L, Bismarck A, Stevens MM and Shaffer MSP, *J Biomed Mater Res A* **88**:65–73 (2009).
9 Xu XB, Li ZM, Shi L, Bian XC and Xiang ZD, *Small* **3**:408–411 (2007).
10 Ye L, Meng XY, Ji X, Li ZM and Tang JH, *Polym Degrad Stab* **94**:971–979 (2009).
11 Lee LJ, Zeng CC, Cao X, Han XM, Shen J and Xu GJ, *Compos Sci Technol* **65**:2344–2363 (2005).
12 Soldano C, Mahmood A and Dujardin E, *Carbon* **48**:2127–2150 (2010).
13 Zhu YW, Murali S, Cai WW, Li XS, Suk JW, Potts JR, *et al*, *Adv Mater* **22**:3906–3924 (2010).
14 Zhang HB, Yan Q, Zheng WG, He Z and Yu ZZ, *ACS Appl Mater Interfaces* **3**:918–924 (2011).
15 Huang X, Yin ZY, Wu SX, Qi XY, He QY, Zhang QC, *et al*, *Small* **7**:1876–1902 (2011).
16 Stankovich S, Dikin DA, Dommett GHB, Kohlhaas KM, Zimney EJ, Stach EA, *et al*, *Nature* **442**:282–286 (2006).
17 Kuilla T, Bhadra S, Yao DH, Kim NH, Bose S and Lee JH, *Prog Polym Sci* **35**:1350–1375 (2010).
18 Nguyen DA, Lee YR, Raghu AV, Jeong HM, Shin CM and Kim BK, *Polym Int* **58**:412–417 (2009).
19 Wang J, Wang X, Xu C, Zhang M and Shang X, *Polym Int* **60**:816–822 (2011).
20 Vadukumpully S, Paul J, Mahanta N and Valiyaveettil S, *Carbon* **49**:198–205 (2011).
21 Verdejo R, Barroso-Bujans F, Rodriguez-Perez MA, de Saja JA and Lopez-Manchado MA, *J Mater Chem* **18**:2221–2226 (2008).
22 Spitalsky Z, Tasis D, Papagelis K and Galiotis C, *Prog Polym Sci* **35**:357–401 (2010).
23 Geim AK and Novoselov KS, *Nat Mater* **6**:183–191 (2007).
24 Rafiee MA, Rafiee J, Wang Z, Song HH, Yu ZZ and Koratkar N, *Acs Nano* **3**:3884–3890 (2009).
25 Xu JZ, Chen T, Yang CL, Li ZM, Mao YM, Zeng BQ, *et al*, *Macromolecules* **43**:5000–5008 (2010).
26 Du JH, Zhao L, Zeng Y, Zhang LL, Li F, Liu PF, *et al*, *Carbon* **49**:1094–1100 (2011).
27 Bui K, Duong HM, Striolo A and Papavassiliou DV, *J Phys Chem C* **115**:3872–3880 (2011).
28 Verdejo R, Saiz-Arroyo C, Carretero-Gonzalez J, Barroso-Bujans F, Rodriguez-Perez MA and Lopez-Manchado MA, *Eur Polym J* **44**:2790–2797 (2008).
29 Pang H, Chen C, Zhang YC, Ren PG, Yan DX and Li ZM, *Carbon* **49**:1980–1988 (2011).
30 Ren PG, Yan DX, Ji X, Chen T and Li ZM, *Nanotechnology* **22**:055705 (8pp) (2011).
31 Gibson LJ and Ashby MF, *Cellular Solids: Structure and Properties*. Cambridge University Press, Cambridge (1999).
32 Indennidate L, Cannoletta D, Lionetto F, Greco A and Maffezzoli A, *Polym Int* **59**:486–491 (2010).
33 Harikrishnan G, Lindsay CI, Arunagirinathan MA and Macosko CW, *ACS Appl Mater Interfaces* **1**:1913–1918 (2009).
34 Solomon MJ, Almusallam AS, Seefeldt KF, Somwangthanaroj A and Varadan P, *Macromolecules* **34**:1864–1872 (2001).
35 Vermant J, Ceccia S, Dolgovskij MK, Mafettone PL and Macosko CW, *J Rheol* **51**:429–450 (2007).
36 Heine DR, Petersen MK and Grest GS, *J Chem Phys* **132**:184509 (6pp) (2010).
37 ten Brinke A, Bailey L, Lekkerkerker H and Maitland GC, *Soft Matter* **3**:1145–1162 (2007).
38 Shen J, Zeng C and Lee LJ, *Polymer* **46**:5218–5224 (2005).
39 Chen L, Ozisik R and Schadler LS, *Polymer* **51**:2368–2375 (2010).
40 Wei T, Luo G, Fan Z, Zheng C, Yan J, Yao C, *et al*, *Carbon* **47**:2296–2299 (2009).
41 Khan U, May P, O'Neill A and Coleman JN, *Carbon* **48**:4035–4041 (2010).
42 Zhang DD, Zu SZ and Han BH, *Carbon* **47**:2993–3000 (2009).

43 Xiang ZD, Chen T, Li ZM and Bian XC, *Macromol Mater Eng* **294**:91–95 (2009).
44 Schaefer DW and Justice RS, *Macromolecules* **40**:8501–8517 (2007).
45 Zhao X, Zhang QH and Chen DJ, *Macromolecules* **43**:2357–2363 (2010).
46 Schniepp HC, Li JL, McAllister MJ, Sai H, Herrera-Alonso M, Adamson DH, *et al*, *J Phys Chem B* **110**:8535–8539 (2006).
47 Lee C, Wei X, Kysar JW and Hone J, *Science* **321**:385–388 (2008).
48 McAllister MJ, Li JL, Adamson DH, Schniepp HC, Abdala AA, Liu J, *et al*, *Chem Mater* **19**:4396–4404 (2007).
49 Sahoo NG, Rana S, Cho JW, Li L and Chan SH, *Prog Polym Sci* **35**:837–867 (2010).
50 Roff WJ, Scott JR and Pacitti J, *Fibres, Films, Plastics and Rubbers: a Handbook of Common Polymers*. Butterworths, London (1971).
51 Cai D, Yusoh K and Song M, *Nanotechnology* **20**:085712 (5pp) (2009).
52 Díez-Pascual AM, Naffakh M, Gomez MA, Marco C, Ellis G, Martínez MT, *et al*, *Carbon* **47**:3079–3090 (2009).
53 Xia HS and Song M, *Soft Matter* **1**:386–394 (2005).
54 Thirumal M, Khastgir D, Singha NK, Manjunath B and Naik Y, *J Appl Polym Sci* **108**:1810–1817 (2008).

